Effect of sildenafil on human aromatase activity: From in vitro structural analysis to catalysis and inhibition in cells

Effect of sildenafil on human aromatase activity:

from *in vitro* structural analysis to catalysis and inhibition in cells

Roberta Baravalle,[1] Francesca Valetti,[1] Gianluca Catucci,[1] Giovanna Gambarotta,[3] Mario Chiesa,[4] Sara Maurelli,[4] Elio Giamello,[4] Ines Barone,[5] Stefania Catalano,[5] Sebastiano Andò,[5] Giovanna Di Nardo,[1,2*] and Gianfranco Gilardi[1,2*]

[1] Department of Life Sciences and Systems Biology, University of Torino, via Accademia Albertina 13, 10123 Torino, Italy

[2] CrisDi, Interdepartmental Center for Crystallography, via Pietro Giuria 7, 10125, Torino, Italy

[3] Department of Clinical and Biological Sciences, University of Torino, Regione Gonzole, 10 - 10043 Orbassano, Italy

[4] Department of Chemistry, University of Torino, via Pietro Giuria 7, 10125, Torino, Italy

[5] Department of Pharmacy, Health and Nutritional Sciences, University of Calabria, Arcavacata di Rende, CS, Italy

[*]Correspondence: giovanna.dinardo@unito.it and gianfranco.gilardi@unito.it

Telephone : +390116704593

Fax : +390116704643

Abstract

Aromatase catalyses the conversion of androgens into estrogens and is a well-known target for breast cancer therapy. As it has been suggested that its activity is affected by inhibitors of phosphodiesterase-5, this work investigates the potential interaction of sildenafil with aromatase. This is carried out both at molecular level through structural and kinetics assays applied to the purified enzyme, and at cellular level using neuronal and breast cancer cell lines.

Sildenafil is found to bind to aromatase with a K_D of 0.58±0.05 μM acting as a partial and mixed inhibitor with a maximal inhibition of 35±2%. Hyperfine sublevel correlation spectroscopy and docking studies show that sildenafil binds to the heme iron via its 6th axial water ligand.

These results also provide information on the starting molecular scaffold for the development of new generations of drugs designed to inhibit aromatase as well as phosphodiesterase-5, a new emerging target for breast cancer therapy.

Keywords : aromatase inhibitors, sildenafil, cytochromes P450, estrogens, breast cancer.

1. Introduction

Aromatase is the cytochrome P450 that converts androgens into estrogens through three catalytic cycles that lead to the aromatization of the A ring of the steroid molecule (Scheme 1A) [1-3].

This protein is directly involved in the control of physiological levels of androgens and estrogens, and it is pathologically over-expressed in breast cancer cells leading to an 'in situ' overproduction of estrogens. Indeed, the enzyme is a very well known target for breast cancer therapy and aromatase inhibitors are used as anticancer drugs since they block the production of estrogens that are responsible for tumour cell proliferation [4]. To date, three generations of aromatase inhibitors have been developed. They are steroidal molecules that accommodate in the active site of the protein mimicking the substrate and, as in the case of the inhibitor exemestane, can cause irreversible inhibition. Non-steroidal inhibitors are azole derivatives containing nitrogen atoms that can directly coordinate to the heme iron. However, aromatase inhibitors can be administrated only in post-menopausal women to avoid the inhibition of ovarian aromatase. In fact, aromatase protein is the product of a single gene and only one isoform is present within different tissues of the human body such as gonads, brain, adipose tissue, placenta, blood vessels, bone, and skin [5]. Such a wide distribution justifies the fact that sex hormones are implicated not only in sexual development and reproduction but also in neurotransmission, immune response [6], cardiovascular and neurological protection [7, 8]. This is the reason why the maintenance of their correct levels is crucial for many physiological and pathological processes. As a consequence, an aromatase inhibitor interferes with the correct balance of sex hormones within the human body, leading in some cases to diseases such as Alzheimer's [9].

Very recently, an overexpression of phosphodiesterase-5 (PDE5) was observed in several cancer tissues and cell lines, including those of the breast and thyroid glands [10, 11]. Moreover, sildenafil that is a cyclic guanosine monophosphate (cGMP)-specific PDE5 inhibitor used for the treatment of erectile dysfunction and pulmonary hypertension [12] has attracted the attention of scientists since different studies have reported that this molecule has a synergic effect with some anti-cancer drugs such as doxorubicin in breast cancer cells [13]. More recently, different studies show that sildenafil blocks the proliferation of colorectal [14] and thyroid cancer cells [11]. Moreover, it was demonstrated that treatment with sildenafil significantly decreases migration and invasion of MCF-7 breast cancer cell line, where PDE5 and aromatase are contemporarily overexpressed [10].

It has been reported that treatment with tadalafil, another PDE5 inhibitor leads to an alteration of testosterone/estradiol ratio in human body that may be due to a modulation of aromatase activity [15]. In another work, it was shown that sildenafil treatment causes an increase in the levels of serum testosterone in male rats [16]. These data suggest that PDE5 inhibitors can act on aromatase as well. The structure of sildenafil shows the presence of a pyrazole ring often involved in aromatase inhibitors, such as anastrozole (Scheme 1 B-C). This paper investigates this hypothesis *in vitro* at molecular level, using the purified N-terminally modified recombinant aromatase (rArom) that we have shown having the same 3D structure of the full-length wild-type human enzyme (RMSD 0.4 Å) [17, 18]. The *in vitro* data are validated using cell models expressing the full-length enzyme, including breast cancer cells.

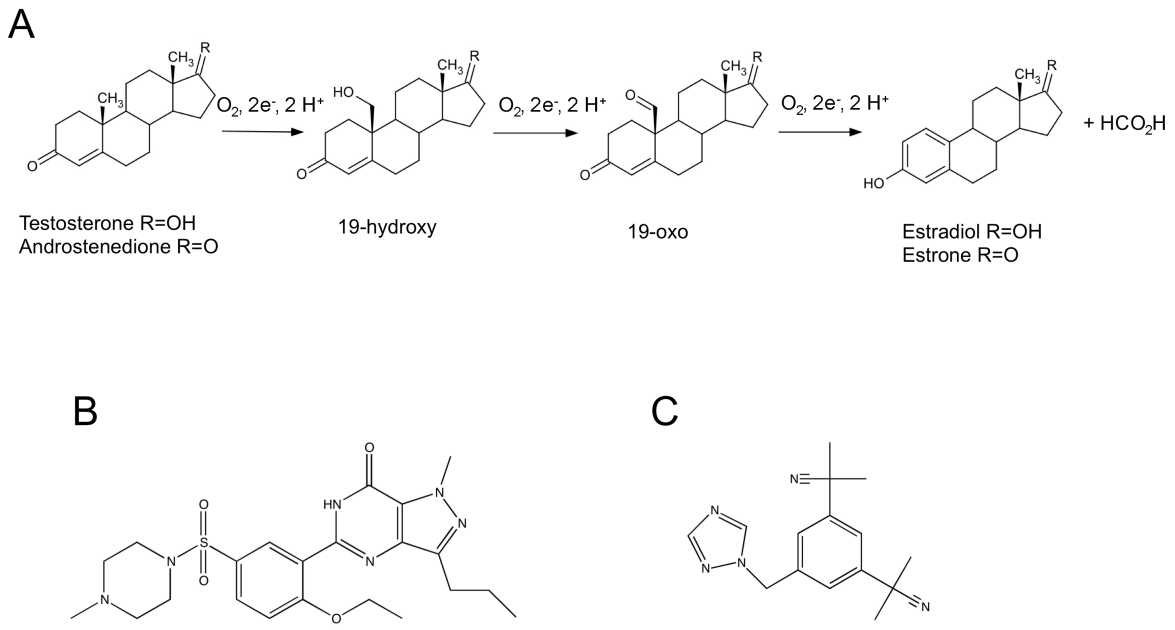

Scheme 1. Structure of substrate, products and inhibitors of human aromatase. A) The three step reaction catalysed by human aromatase; B) chemical structure of sildenafil and C) chemical structure of the aromatase inhibitor anastrozole.

2. Materials and methods

2.1 Materials

All the chemicals were purchased from Sigma Aldrich and were analytical grade. 19-oxoandrostenedione was purchased from ABI Chem (Germany). Human recombinant cytochrome P450-reductase (CPR) was purchased by Life Technologies.

2.2 Protein expression and purification

Recombinant human aromatase (rArom) was expressed and purified as previously described [19]. Briefly, *E. coli* DH5α rubidium-competent cells were transformed by a pCW Ori+ vector carrying an IPTG-inducible Tac promoter, an ampicillin resistance gene and rArom cDNA. Positive clones selected by 100 µg/mL ampicillin were grown in Terrific Broth (TB). Expression was induced by 0.5 mM IPTG and cells were let grown 48 hours at 28°C in the presence of the heme precursor δ-aminolevulinic acid.

Cells were harvested and re-suspended in a 100 mM KPi pH 7.4, 20% glycerol, 0.1 % Tween-20 and 1 mM β-mercaptoethanol buffer supplemented with 1 mg/mL lysozyme, 1% Tween-20 and 1 mM PMSF at 4°C, disrupted by sonication and ultra-centrifuged for 25 minutes at 40,000 rpm and 4°C in a Beckman Coulter Ultra centrifuge. rArom was purified by loading the supernatant on a diethylaminoethyl ion-exchange column (DEAE-Sepharose Fast-Flow, GE Healthcare) followed by a Nickel-ion affinity column (Chelating-Sepharose Fast-

Flow, GE Healthcare). The protein was eluted applying a linear histidine gradient from 1 to 40 mM. The fractions containing the enzyme were pooled and histidine was removed in Amicon Ultra 30,000 MWCO devices (Millipore).

2.3 UV-vis spectroscopic studies.

The binding of rArom to sildenafil was studied as a spectroscopic shift of the γ Soret peak from 418 nm to 422 in an Agilent 8453 UV-vis spectrophotometer (diode array) at the controlled temperature of 25°C (Agilent 89090 A Peltier). The rArom protein (2.0 μM) was titrated with increasing sildenafil concentrations (0.26 μM-2.5 μM) in 100 mM KPi pH 6.5, 7.0, 7.4, 8.0 and 100 mM Tris-HCl pH 8.5 and 9.0 supplemented with 262 mM NaCl to keep the ionic strength constant. All buffers contained also 20% glycerol, 0.1% Tween-20 and 1 mM β-mercaptoethanol. Spectral transitions (ΔAbs_{422} - ΔAbs_{418}) were plotted as a function of sildenafil concentration and the data fitted to the following equation:

$$(\Delta Abs_{422} - \Delta Abs_{418}) = [(\Delta Abs_{422} - \Delta Abs_{418})_{MAX}\, L_{FREE}]/(K_D + L_{FREE})$$

where L_{FREE} is L total-[EL] and [EL] = $(\Delta Abs_{422} - \Delta Abs_{418})[E]/(\Delta Abs_{422} - \Delta Abs_{418})_{MAX}$ and K_D the dissociation constant. Four independent measurements were averaged and error bars represent the standard deviation.

2.4 EPR studies

X-band CW EPR spectra were recorded at 77K on a Bruker EMX spectrometer (microwave frequency 9.47 GHz) equipped with a cylindrical cavity. A microwave power of 10 mW, modulation amplitude of 0.3 mT and a modulation frequency of 100 KHz were used.

Pulse EPR experiments were performed on an ELEXYS 580 Bruker spectrometer (at the microwave frequency of 9.76 GHz) equipped with a liquid-helium cryostat from Oxford Inc. The magnetic field was measured by means of a Bruker ER035M NMR gauss meter. All pulse EPR experiments were performed at 7K.

Electron-spin-echo (ESE) detected EPR experiments were carried out with the pulse sequence: $\pi/2 - \tau - \pi - \tau$–echo, with microwave pulse lengths $t_{\pi/2}$ = 16 ns and t_{π} = 32 ns and a τ value of 160 ns.

Hyperfine Sublevel Correlation (HYSCORE) experiments [20] were carried out with the pulse sequence $\pi/2 - \tau - \pi/2 - t_1 - \pi - t_2 - \pi/2 - \tau$ – echo with the microwave pulse lengths $t_{\pi/2}$ = 16 ns and t_{π} = 32 ns. The time intervals t_1 and t_2 were varied in steps of 16 ns starting from 96 ns to 4704 ns. A τ value of 176 ns was chosen. A shot repetition rate of 1 kHz was used. A four-step phase cycle was used for eliminating unwanted echoes. The time traces of the HYSCORE spectra were baseline corrected with a third-order polynomial, apodized with a Hamming window and zero filled. After two-dimensional Fourier transformation, the absolute value spectra were calculated. Both CW and HYSCORE spectra were simulated using the Easyspin program [21].

Typical rArom concentrations adopted for the EPR analysis were 0.5 mM.

2.5 Molecular docking

The drug sildenafil was docked into the crystal structure of rArom (PDB ID 4KQ8), where the substrate was removed before docking. The YASARA embedded AutoDock V4 algorithm [22] was used to predict protein-ligand interactions. In order to dock the ligands in the protein active site, a simulation cell (15x15x15 Å) was built around the heme iron atom and 25 runs of local docking were performed allowing ligand and protein flexibility. The binding energies were predicted using the scoring function included in AutoDock. The binding energy is obtained by calculating the energy at infinite distance (between the selected object and the rest of the scene, i.e. the unbound state) and subtracting the energy of the scene (i.e. the bound state). The more positive the binding energy, the more favorable the interaction.

In a second simulation, the pentacoordinated heme cofactor was replaced by the water-bound hexacoordinated one from the crystal structure of CYP106A2 (PDB ID 4YT3) [23] and docking was again performed.

In a third simulation, the drug sildenafil was globally docked into aromatase in the presence of androstenedione to check the presence of a second binding site.

2.6 Activity assay and product quantification by HPLC

For the determination of the kinetics parameters and the inhibition constants for the three steps of reaction, the enzymatic conversion was followed through the separation and quantification of the substrate and the product formed by HPLC.

Reactions were set up by mixing 250 nM of rArom and 250 nM of cytochrome P450 reductase (CPR), increasing concentrations of the three androgens (0.5 µM-300µM) and 0.5 mM NADPH up to 100 µL in a 100 mM KPi pH 7.0, 20% glycerol, 0.1% Tween-20 and 1 mM β-mercaptoethanol buffer. Reactions were carried out for 10 minutes at 30°C, heat-inactivated for 10 minutes at 90°C and centrifuged for 5 minutes at 11,000 *g*. Reactions in the presence of sildenafil were set up as described above with an initial incubation for 5 minutes at 25°C of rArom and 6.7 µM of the drug.

After centrifugation, the supernatant was collected and injected into the HPLC system. Reaction products formed by rArom were analysed in a 1200 series HPLC apparatus (Agilent Technologies) using a ZORBAX Eclipse Plus C18 reverse phase column (Agilent Technologies).

Analytes were eluted applying an acetonitrile HPLC grade (Sigma Aldrich) linear gradient (5%-100%) mixed to filtered and degased MilliQ water at the flow rate of 0.5 mL/min.

The androgens androstenedione (AD), 19-hydroxyandrostenedione (19-OHAD) and 19-oxoandrostenedione (19-OXOAD and estrone were detected by a diode array detector set at the wavelengths of 237 nm and 280 nm, respectively.

Different concentrations of 19-hydroxyandrostenedione (0.5 µM-100 µM), 19-OXOandrostenedione (0.5 µM - 300 µM) and estrone (0.2 µM-10 µM) were dissolved in a 100 mM KPi pH 7.0, 20% glycerol, 0.1% Tween-20 and 1 mM β-mercaptoethanol buffer to be injected into the HPLC system to build a calibration curve. The peaks were integrated and the corresponding areas plotted as a function of the standard concentration resulting in a linear regression curve used for the quantification of aromatase reaction products. Four independent measurements were averaged and the standard deviation calculated. Data fitting were performed by Sigma Plot

9.0 software. The inhibition constants K_{EI} and K_{EIS} were calculated using the following equation developed for partial inhibitors [24]:

$1/V = [(K_M/V_{max}) \times B \times 1/S] + A/ V_{max}$,

where $B = 1 + ([I]/K_{EI})$ and $A = 1 + ([I]/K_{EIS})$.

2.7 Activity assay and product quantification by estrone-ELISA

When considering estrone as the only final biologically relevant product, a more sensitive direct competitive ELISA estrone Kit (Diagnostic Biochem Canada Inc.) was used to quantify aromatase activity.

This assay was used to quantify aromatase product to calculate the inhibition percentage and the for sildenafil using the purified enzyme.

Reactions were set up by mixing 15 nM of rArom and CPR, increasing sildenafil concentrations (25 nM-400 nM), 10 µM androstenedione and 0.5 mM NADPH up to 60 µL in a 100 mM KPi pH 7.4, 20% glycerol, 0.1% Tween-20 and 1 mM β-mercaptoethanol buffer. Reactions were carried out for 10 minutes at 30°C, heat-inactivated for 10 minutes at 90°C and centrifuged for 5 minutes at 11,000 *g* prior performing ELISA following the manufacturer instructions.

The IC_{50} for sildenafil was calculated according to the following equation built for partial inhibitors:

$A = [(A_{max} - A_{min})/ 1 + ([I]/IC_{50})] + A_{min}$,

where A is the activity percentage of the enzyme in the presence of the inhibitor at the concentration [I], A_{max} is the activity when the inhbitor is absent (set at 100%) and A_{min} is the activity percentage that can be obtained at the highest inhibitor concentrations [25].

Estrone-ELISA was also used to quantify aromatase reaction product when using the ST14A cell line.

2.8 ST14A neuronal cell culture and transient transfection

The eukaryotic neuronal cell model used to test the effect of sildenafil on full-length transmembrane aromatase was the neural progenitor cell line ST14A [26] Cells were grown as monolayers in Dulbeccos's Modified Eagle Medium (DMEM) supplemented with 100 units/ml penicillin, 0.1 mg/ml streptomycin, 1 mM sodium pyruvate, 2 mM L-glutamine, and 10% heat-inactivated fetal bovine serum (FBS; Invitrogen), at the permissive temperature of 33°C in a 5% CO_2 atmosphere saturated with H_2O.

Confluent adherent cells grown in 10 cm diameter dishes were transiently transfected in Opti-MEM reduced serum medium (Gibco) by mixing 10 µg of the expression vector pCMV6-XL4 carrying the cDNA coding for the full-length aromatase (Origene, Rockville, USA) or a control empty vector (pIRES-puro2) and 10 µL of Lipofectamine2000 (Invitrogen) according to the manufacturer recommendations.

24 hours post-transfection cells were split in 6 cm diameter dishes to carry out the following analysis with cells derived from the same transient transfection. 48 hours after transfection cells were firstly treated with four different sildenafil concentrations (25 nM, 75 nM, 200 nM and 1 µM) in DMEM serum-free at 33°C, 5% CO_2 atmosphere for ten minutes and subsequently stimulated in DMEM serum-free supplemented with the same sildenafil concentrations and 50 nM androstenedione at 33°C, 5% CO_2 atmosphere for ten minutes; cells stimulated with 50 nM androstenedione only were used as control. The estrone containing supernatant was

collected and analysed by direct competitive ELISA estrone Kit (Diagnostic Biochem Canada Inc.) following manufacturer instructions.

2.9 Protein extraction and Western blot analysis

Total proteins were extracted 48 hours after transient transfection by solubilizing cells in boiling Laemmli buffer (2.5% SDS and 0.125 M Tris-HCl pH 6.8), followed by 5 min denaturation at 100 °C in 240 mM 2-mercaptoethanol and 18% glycerol. Western blot analysis was carried out as previously described [27]. Proteins (40 µg/sample) were resolved by 8% SDS-PAGE and transferred to a HybondTM C Extra membrane (Amersham Biosciences) following the manufacturer instructions. For immunoblotting on ST14A neuronal cells a rabbit primary polyclonal antibody anti-GAPDH (Thermo Fisher) and a rabbit primary polyclonal anti-aromatase antibody kindly provided by Dr Harada (Fujita Health University, Nagoya, Japan) were used diluted 1:1,000 in TBST 1X (150 mM NaCl, 10 mM Tris-HCl pH 7.4, 0.1% Tween-20) supplemented with 5% bovine serum albumin; as secondary antibody a horseradish peroxidase-conjugated goat anti-rabbit (GE Healthcare) was used diluted 1:20,000 in TBST 1X supplemented with 5% bovine serum albumin.

2.10 Generation of MCF-7 Arom breast cancer cells

MCF-7 breast cancer cells stably overexpressing aromatase (MCF-7 Arom cells) were previously generated in our laboratories [28]. Briefly, MCF-7 cells were stably transfected with the pZeo-Arom expression vector containing full-length human aromatase cDNA using Fugene 6 reagent according to the manufacturer (Roche), and individual clones were isolated and expanded with Zeocin selection. Stably transfected clones were screened for expression of aromatase using immunoblot analysis and for enzymatic activity by tritiated water release assay. Cells were routinely maintained in minimal essential medium (MEM) supplemented with 10% fetal bovine serum, 0.1 nmol/l nonessential amino acid, 2 mmol/l L-glutamine, 50 units/ml penicillin/streptomycin, and 0.2mg/ml Zeocin.

2.11 Tritiated water release assay

The tritiated water release assay [29] was used to quantify the tritiated water released from [1β-3H]androst-4-ene-3,17-dione (Perkin Elmer) after aromatization to estrone in the experiment with MCF7 breast cancer cells.
Briefly, MCF-7 Arom breast cancer cells were treated for 10 minutes with vehicle or four different sildenafil concentrations (25 nM, 75 nM, 200 nM and 1 µM) in serum-free DMEM/F-12 medium. The aromatase activity in subconfluent MCF-7 Arom cell culture medium was measured by the tritiated water release assay using 0.5 µM of radiolabeled androstenedione as substrate [29]. The incubations were performed at 37° C for 1 h under an air-CO_2 (5%) atmosphere. The results obtained were normalized to mg of protein and expressed as % of residual aromatase activity.

3. Results

3.1 UV-vis spectroscopic analysis of sildenafil binding to human aromatase

The effect of a ligand on a cytochrome P450 can be monitored as a spectroscopic shift of the enzyme maximum absorbance γ band (Soret peak) in the absorbance visible region. In the resting state, the heme iron of

cytochromes P450 is hexa-coordinated and a water molecule acts as sixth ligand leading to a maximum of absorbance at 417-419 nm [30]. The binding of a ligand to the active site of a cytochrome P450 can have two distinct effects. The so-called type I ligands displace the water molecule with a consequent low-to-high spin transition of heme iron that becomes penta-coordinated. This is spectroscopically detectable as a shift of the maximum absorbance peak from 417-419 nm to 390-394 nm [31]. On the other hand, type II ligands are nitrogen-containing compounds that displace the water molecule while directly coordinating to the heme iron, or alternatively they form a hydrogen bond with the water molecule present as the sixth ligand [32-34]. In the case of type II ligands, the heme iron is hexa-coordinated and the maximum absorbance peak shift from 418 nm to 422-426 nm [35]. On this basis, the binding of sildenafil to human aromatase was investigated by following the effect of its addition on the absorption properties of heme iron.

When the visible spectra of rArom (2 μM) were recorded before and after the addition of 2.5 μM of sildenafil, a small effect on the γ Soret peak was observed, with a shift from 418 to 422 nm (Figure 1A). This change is also evidenced in the difference spectra with a decrease of the absorbance at 412 nm and a concomitant increase at 434 nm (inset Figure 1A). This spectroscopic behaviour is usually ascribed to the so-called type II ligands of cytochromes P450 [30, 32, 33] and it was previously observed also for rArom in complex with the known inhibitor anastrozole [34, 36]. In contrast, rArom in complex with the substrate androstenedione and the steroidal inhibitor exemestane give rise to type I spectra, consistent with the displacement of the sixth water ligand of the heme iron [36].

Titrations with increasing amounts of sildenafil (0.26-2.5 μM) led to the construction of a binding curve with a typical hyperbolic trend (Figure 1B). Fitting the experimental data to a one-site saturation led to a K_D of 0.58 ± 0.05 μM at pH 7.0. This value is within the same range of the K_D calculated for the binding of the substrate androstenedione and the inhibitor anastrozole [19]. The K_D values for sildenafil in the pH rage from 6.5 to 9.0 did not show a linear increase as a function of pH (Supplemental information, Table S1), as previously reported for the substrate androstenedione [36].

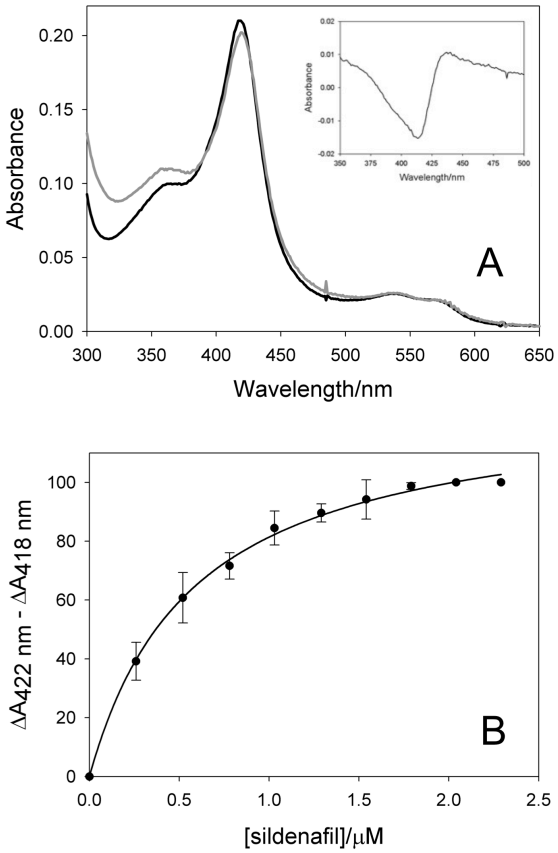

Figure 1. UV-vis spectroscopy shows a Type II binding of sildenafil to human aromatase. A) Visible direct spectra of ligand-free rArom (solid black line) and in the presence of 2.5 μM of sildenafil (solid grey line). Inset: difference spectrum of rArom bound to sildenafil minus ligand-free rArom. B) Binding curve of sildenafil.

3.2 EPR spectroscopy

Since the spectral features of rArom-sildenafil complex are similar to those previously observed for rArom-bound to anastrozole [34, 36], the possibilities to have or a direct N-Fe bond formation (as in the case of anastrozole) either a hydrogen bond *via* a water molecule was investigated by EPR spectroscopy.

The binding of sildenafil in the active site of aromatase was studied by continuous wave (CW) and pulse EPR experiments at 77 K on the enzyme co-purified with sildenafil at pH 7.4 (experiments performed at pH 7.0 are shown in Supplemental information). The results are compared to those previously obtained on ligand-free aromatase and on the protein in complex with the known inhibitor anastrozole [34].

Figure 2A shows the X-band CW EPR spectra recorded for the different samples. All the spectra are dominated by the typical powder pattern of low-spin (S= ½) Fe(III) heme centers. The comparison shows that the spectrum of aromatase co-purified with sildenafil (Figure 2Aa 2Ac) is slightly different from both the substrate-free aromatase (Figure 2Aa) and the aromatase co-purified in presence of anastrozole (Figure 2Ab). As ascertained by computer simulations (dotted lines in Figure 2A), the EPR spectrum of the substrate free aromatase indicates the presence of two different species characterized by slightly different g factors (S1: g_1=1.899; g_2=2.254; g_3=2.493 and S2: g_1=1.924; g_2=2.254; g_3=2.415) (Supplemental data, Table S2) in accordance with the

multiplicity of species already observed for other P450 proteins [37, 38]. Upon binding of both inhibitors, a change in the CW EPR spectrum is observed, with the selective suppression of one of the two EPR active species. In particular, upon binding of anastrozole, species S2 is suppressed (Figure 1A, (b)) while the contrary is observed in the case of sildenafil. The spectra are found to be practically independent on the pH of the solution (Supplemental information, Figure S1).

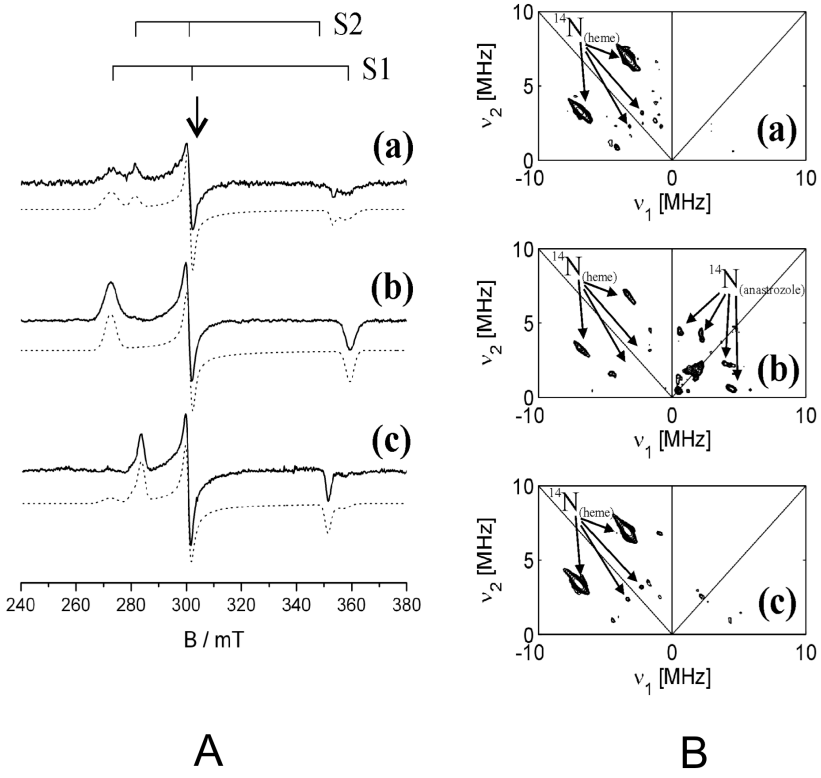

Figure 2. EPR spectroscopy shows a different binding mode of sildenafil compared to the known inhibitor anastrozole. (A) Experimental (full line) and simulated (dotted line) X-band CW-EPR of aromatase. (B) Experimental HYSCORE spectra at the field position corresponding to the arrow in (A) ($B_0 \cong 310.5$ mT). The spectra in (A) and (B) refer to frozen solutions of (a) substrate-free aromatase, (b) aromatase co-purified with anastrozole and (c) aromatase co-purified with sildenafil at pH = 7.4. The arrows in the HYSCORE spectra indicate the signals belonging to porphyrin nitrogen nuclei of heme rings and axial ligated nitrogen nuclei in anastrozole.

In order to ascertain the chemical environment of the active sites in the various samples, X-band HYSCORE spectra were recorded at different magnetic field positions (Figure 2B and Supplemental data, Figure S2 and S3). The spectra of all three samples are dominated by cross peaks in the (-,+) quadrant due to the typical interactions of the unpaired electron localized on the Fe(III) centers with the nitrogen nuclei of the porphyrin ring (Figure 2B (a), (b) and (c)) [34, 39, 40]. Proton ridges are also present in all spectra, which are not assigned due to the large number of potential contributors. As reported before [34], the HYSCORE spectrum recorded upon addition of anastrozole (Figure 1B (b)) shows additional peaks in the (+,+) quadrant. These signals have been assigned to the N4 nitrogen of the triazole ring of anastrozole, demonstrating the formation of a chemical bond between the ferric heme center and the molecular inhibitor. Under the same circumstances, no such evidence is observed

when aromatase is co-purified with sildenafil (Figure 2B (c)), suggesting a different interaction mechanism.

3.3 Effect of sildenafil on the catalytic parameters of rArom

In order to understand the effect of sildenafil on the three different steps of aromatase reaction, steady state kinetics through quantification of the reaction products by HPLC analysis were carried out using androstenedione (AD), 19-hydroxyandrostenedione (19-OHAD) or 19-oxoandrostenedione (19-OXOAD) as starting substrates. The activity of rArom (55 nmol/min/mg protein) [17] was previously demonstrated to be comparable to the full-length placental and crystallized enzyme [18] as well as other recombinant systems previously developed for the same enzyme [41-45].

First, it was assessed that the product formation rate was linear during the first 10 minutes at 30°C for all the three compounds used as starting substrates (AD, 19-OHAD and 19-OXOAD). After this time, the reactions were stopped by heat, centrifuged and the supernatant directly injected into the HPLC column. A typical chromatogram obtained from a reaction mixture containing 7 μM of the substrate androstenedione in the absence and presence of 6.7 μM of sildenafil is shown in Supplemental data, Figure S4.

Figure 3 shows the plots of the product formation rates as a function of the concentration of the starting substrate. These plots take into account the amounts of the intermediates formed (when present) and of the final product estrone. Data were fitted to the Michaelis-Menten equation and the catalytic parameters are reported in Table 1.

When the overall reaction (three steps) or the last two steps are considered, an increase of K_M and a decrease of the V_{max} are observed in the presence of sildenafil, indicating that sildenafil acts as a mixed inhibitor, as demonstrated also by Lineweaver-Burk plots (insets in Figure 3).

When only the last aromatization step is considered, an atypical trend is observed in the presence of sildenafil, similar to a sigmoidal-cooperative curve. However, the Hill plot shows that a cooperative effect should be excluded, since the experimental data lie on two different linear curves with a Hill coefficient of 1.2 and 1.1, respectively (Figure 3D). In the range 0-20 μM of 19-OXOAD, a linear growth of the product estrone is obtained as the 19-OXOAD concentration increases (Figure 3C). In the concentration range 20-300 μM of 19-OXOAD, a hyperbolic trend is observed. When the data within this range of concentrations are fitted by a Michaelis-Menten curve, an increase of the K_M value is observed when sildenafil is present while the V_{max} is unaltered, suggesting a competitive effect of the drug in this last step of reaction (Table 1).

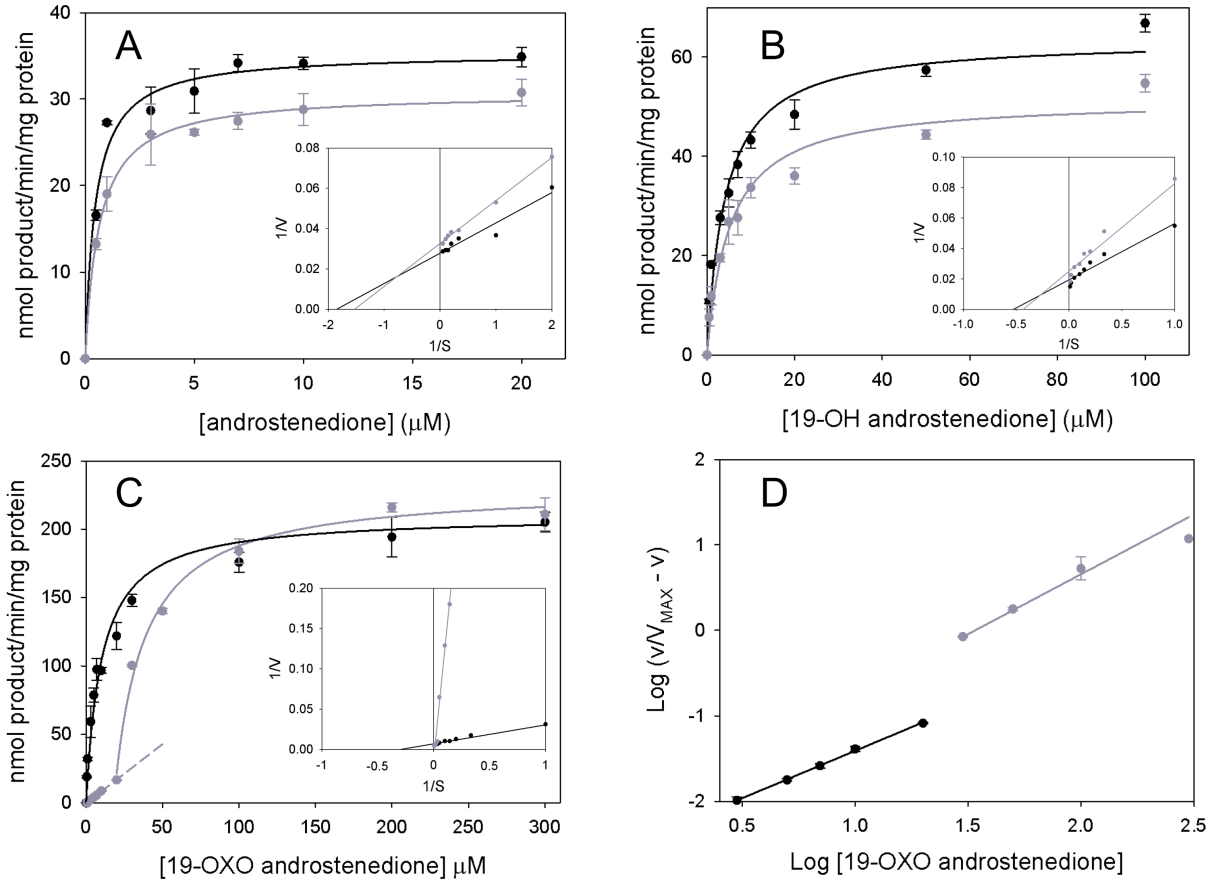

Figure 3. The kinetic parameters of the three steps of reaction of rArom are affected by the presence of sildenafil. rArom kinetic curves in the absence (black circles) and in the presence (grey circles) of sildenafil using as starting substrates A) androstenedione (AD), B) 19-hydroxyandrostenedione (19-OHAD) and C) 19-oxoandrostenedione (19-OXOAD). Insets show the corresponding Lineweaver-Burk linearization curves. D) Hill linearization plot for the kinetics of 19-OXOAD (data from panel C) and fitting to linear curves.

Table 1 reports the K_{EI} and K_{EIS} values obtained for the three steps of reaction. When considering the overall reaction, the K_{EI} value is lower than that of K_{EIS}, suggesting that sildenafil can bind both the enzyme and the enzyme-substrate complex with a higher affinity for the first one, as supported by docking experiments (see section 3.4).

Moreover, the K_{EI} measured for 19-OXOAD is the lowest calculated, suggesting that, when considering the overall reaction, the last step is the limiting one in terms of inhibition, with a significant competitive effect of sildenafil towards 19-OXOAD.

3.4 Docking of sildenafil in the active site of aromatase

In order to add structural insights to the functional data about the molecular interaction between sildenafil and aromatase, docking simulations were performed using the crystal structure of the recombinant enzyme (PDB ID 4KQ8) where the substrate androstenedione was removed. The drug sildenafil reaches and accommodates into

the active site of the protein with a binding energy of 9.3 kcal/mol (site A). Moreover, the molecule does not interact through hydrogen bonds with Asp309, the proton donor for the third step of reaction [36] explaining the non-linear trend observed for the K_D values for sildenafil as a function of pH previously observed for the substrate androstenedione [36]. Since sildenafil acts as a type II ligand and, according to the simulations, nitrogen atoms are far away from the iron atom, the possibility to have a hydrogen bond formation of the drug with the water molecule present as sixth axial ligand was investigate by docking sildenafil in the crystal structure of rArom where the pentacoordinated heme cofactor was replaced by the water-bound hexacoordinated one. The best pose is shown in Figure 4A and the drug binds with a energy of 8.5 kcal/mol and it almost completely overlaps with the previous docking run (rmsd 1.13 Å). Moreover, a hydrogen bond between the water molecule coordinating the heme iron and an oxygen atom of the drug is predicted since their distance is 2.3 Å.

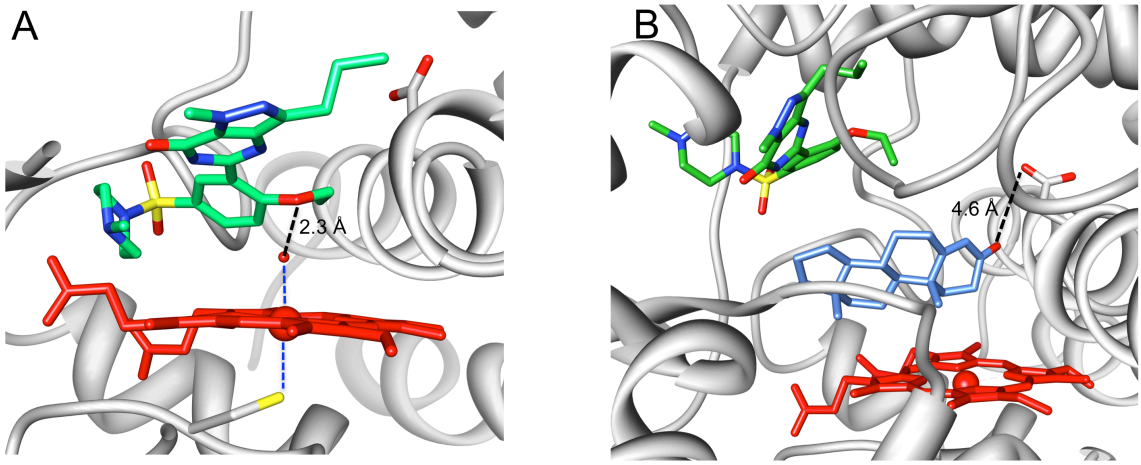

Figure 4. Sildenafil docks into the active site of human aromatase. Docking was performed in the following two conditions: A) the androstenedione substrate is removed and the pentacoordinated heme cofactor is replaced by the water-bound hexacoordinated one (red) B) the enzyme is in complex with the substrate androstenedione (blue) as in the original X-ray structure.

Since a partial and mixed inhibition was observed, the coexistence of the substrate androstenedione and the drug was also investigated by docking sildenafil in the substrate-bound crystal structure (Figure 4B). The drug can accommodate in an alternative site (site B) with a binding energy of 11.2 kcal/mol when the substrate is present. However, as shown by docking simulations, the presence of the drug may affect the positioning of the substrate in the active site moving the keto oxygen atom of the A-ring too far away from Asp309 (4.6 Å) to form the hydrogen bond and to accept the proton in the third catalytic step.

3.5 IC_{50} measurements under physiological substrate concentrations

The physiological concentration of estrone is in the nM range and the circulating concentration of sildenafil has been reported to vary from 100 to 800 nM [46,47]; therefore, a more sensitive ELISA method for estrone detection and quantification was used to evaluate the inhibitory effect of the drug on rArom activity and to calculate the IC_{50} in conditions mimicking the physiological parameters.

The activity of rArom in the presence of a fixed substrate concentration (10 μM) and different amounts of sildenafil (from 25 to 400 nM) was measured and a partial inhibitory effect was obtained up to 35±2 % in the presence of 400 nM of the drug (Figure 5). Even increasing the drug concentration, the activity was not further decreased suggesting that sildenafil acts as a partial inhibitor. This is confirmed by the plot of 1/V versus the inhibitor concentration showing an hyperbolic rather than a linear trend (inset Figure 5) [24]. From the dose-response curve shown in Figure 5, an IC_{50} of 47 ± 1 nM where IC_{50} is actually the concentration where half of the maximal inhibition (i.e. 17.5 % in absolute percentage) is observed.

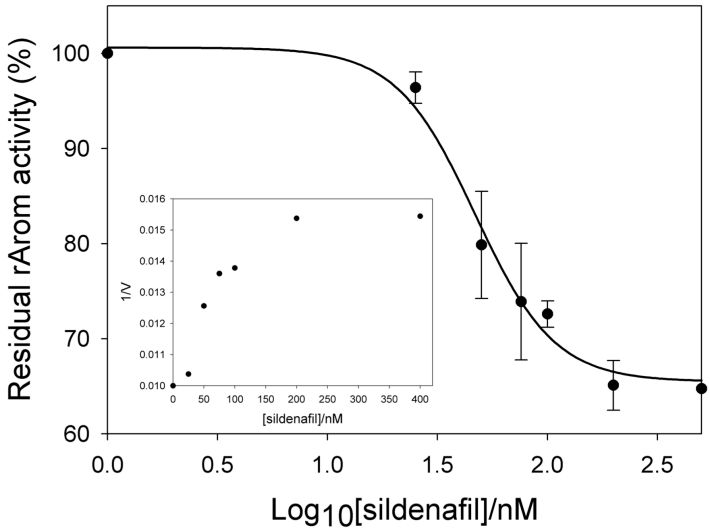

Figure 5. Dose-response curve for rArom activity in the presence of increasing sildenafil concentrations. Inset: Dixon plot showing a hyperbolic trend typical of partial inhibitors.

3.6 Effect of sildenafil on full-length aromatase activity in cells

Like the other mammalian cytochromes P450, human aromatase is bound to the membrane of the endoplasmic reticulum through a N-terminal fragment. The N-terminal portion anchoring the protein to the membrane needs to be removed when a recombinant expression system is developed. However, the access channel of the protein has been suggested to be at the membrane-cytoplasm interface leading to a higher solubility of the steroid substrates and inhibitors [18]. In order to verify the inhibitory effect of sildenafil in cells expressing full-length aromatase inserted in the membrane, we first used as cell experimental model human MCF-7 breast cancer cell line stably overexpressing aromatase (MCF-7 Arom cells), on the basis of the relevance of aromatase in breast tumour progression. This cell line has been previously generated in our laboratories to study aromatase inhibitor response [28], and these cells were found to overexpress aromatase with an activity approximately 1,000 times higher than cells transfected with control vector (20 versus 0.022 pmol/h/mg protein, respectively). Cells were treated for 10 minutes with vehicle or different amounts of sildenafil reported to the circulating ones [47] and aromatase activity was assessed by tritiated water release assay. Interestingly, we observed that sildenafil significantly inhibited aromatase activity in a dose-dependent manner, inducing about 38% of decrease at 1 μM of concentration (Table 2). Moreover, on the basis of the relevance of aromatase protein in neural cells, where

estrogens have been demonstrated to act as neurotransmitters [48] and to be neuroprotective [49], as additional model of analysis we used the neural progenitor ST14A cell line. Cells were transfected with an aromatase expression vector and protein expression was confirmed by Western blotting analysis (Figure 6). Aromatase activity after 40 hours from transfection resulted to be about 150 times higher than cells transfected with the control vector (10.1 versus 0.07 pmol/hour/mg proteins, respectively).

Aromatase activity was then assayed in presence of increasing concentrations of sildenafil. After 10 minutes of treatment, the supernatant was collected and estrone quantified by estrone ELISA in ST14A aromatase-expressing cells. As previously shown for human breast cancer cells, we also observed a dose-response effect in aromatase-transfected ST14A cells, with the maximal inhibition of approximately 35% at the highest concentration of 1 μM (Table 2).

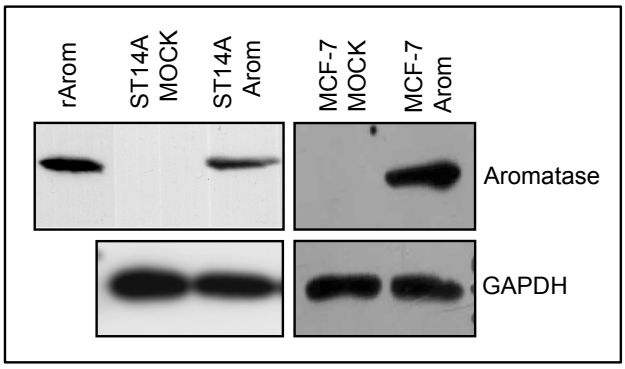

Figure 6. Western blot analysis performed on total cellular proteins extracted from ST14A neuronal cells transiently transfected with full-length aromatase and from parental MCF-7 breast cancer cells stably transfected with full-length aromatase. GAPDH was used as house-keeping protein. Purified rArom was used as positive control.

4. Discussion

The effect of sildenafil on human aromatase activity is studied by a combination of techniques that give information about how this drug can bind in the active site of the protein at molecular level and how it can interfere with the three steps reaction both at molecular and cellular levels.

The binding of sildenafil is studied by UV-vis and EPR spectroscopic techniques, showing that the drug is able to access the active site of the enzyme behaving as a type II cytochrome P450 ligand. The CW EPR spectra of aromatase co-purified in presence of sildenafil with respect to pure aromatase (Figure 2A) suggest a meaningful modification in the local geometry of the active site induced by the presence of sildenafil. Unlike the case of anastrozole, the HYSCORE spectra indicate that no direct nitrogen coordination is present. However, the typical spectroscopic transitions of type II ligands can arise from a hydrogen bond between the drug and the water molecule present as sixth ligand for the heme iron [32]. Docking simulations indicate that such a bond can form between the oxygen atom of the ethoxy moiety of the drug and the water molecule mentioned above that is not displaced from iron coordination. Such a weak interaction, compared to the one observed for aromatase inhibitors where a nitrogen atom directly coordinates the heme iron [34], justifies the partial inhibition effect

exerted by sildenafil. In this case, the drug can be displaced by the substrate more easily than other inhibitors such as anastrozole. However, the K_D values measured by the spectroscopically detectable spin transition of the heme iron induced by sildenafil are in the same range as those calculated for the substrate androstenedione and the inhibitor anastrozole [36]. Moreover, we previously demonstrated that the binding of the substrate androstenedione is dramatically affected by pH, with a K_D increasing as the pH varies from 6.5 to 9.0 and it was not possible to see a substrate-induced spin shift at pH higher than 9.0. This behaviour was assigned to a specific residue (Asp309) by site directed mutagenesis experiments [36]. According to the crystal structure, this residue is involved in a hydrogen bond with the keto-group of the substrate and it is protonated at physiological pH [17, 18, 36]. For the aromatase inhibitor anastrozole, the K_D values variation did not show a linear increasing trend in the pH range 6.5-9.0, indicating that the inhibitor binding does not directly depends on the protonation state of Asp309 in the pH range investigated.

The access of the drug into the active site of human aromatase alters the kinetic parameters that were studied for all the three steps of reaction. In particular, the effect of sildenafil on the three K_M values is more relevant on 19-OXOAD, the compound that also shows the highest K_M compared to the substrate AD and the first intermediate 19-OHAD. An overall mixed inhibition effect can be observed taking into account also the first and the second reaction steps that can be explained with the presence of a second binding site for sildenafil. Docking simulations confirm that sildenafil can bind in an alternative site (site B) affecting the positioning of the substrate in the catalytic pocket where the keto oxygen atom of the steroid A-ring moves too far away from Asp309 (4.6 Å) to form the hydrogen bond and thus accept the proton for the third catalytic step. The presence of two potential sites for sildenafil binding may explain the mixed inhibitory effect exerted by the drug on aromatase activity.

In cells, the plasmid carrying the full-length human aromatase gene is transfected and the enzyme contains the N-terminal helix anchoring the protein to the membrane. Thus, aromatase activity is measured on the enzyme working in its physiological environment where the solubility and the bioavailability of substrates and inhibitors can be affected. Even in these cases, a partial inhibitory effect is observed on the production of estrogens. However, when introducing cell models, it has to be taken into account that many different parameters such as the lower aromatase physiological concentration can complicate the scenario. For example, in cells, sildenafil blocks PDE5 and increases the levels of cGMP that is an activator of the protein kinase G (PKG). PKG along with other kinases may modulate aromatase activity through phosphorylation processes, as already previously reported [50].

5. Conclusion

In conclusion, due to growing evidence about the benefits of PDE5 inhibitors as anticancer drugs [51] and about PDE5 as a new potential target for breast cancer therapy [10], the results of this work can be interesting since they can offer the basis to develop a new generation of inhibitors that combine old (aromatase) and new (PDE5) targets for breast cancer therapy.

Funding

This work was supported by the FIRB grant 2012 Programme “Futuro in Ricerca” project RBFR12FI27_004 to Giovanna Di Nardo and RBFR12FI27_001 to Ines Barone).

References

[1] E.A.J. Thompson, P.K. Siiteri, The involvement of human placental microsomal cytochrome P-450 in aromatization, J. Biol. Chem. 249 (1974) 5373-5378.

[2] E.R. Simpson, M.S. Mahendroo, G.D. Means, M.W. Kilgore, M.M. Hinshelwood, S. Graham-Lorence, B. Amarneh, Y. Ito, C.R. Fisher, M.D. Michael, Aromatase cytochrome P450, the enzyme responsible for estrogen biosynthesis, Endocr. Rev. 15 (1994) 342-355.

[3] G. Di Nardo, G. Gilardi, Human aromatase: perspectives in biochemistry and biotechnology, Biotechnol. Appl. Biochem. 60 (2013) 92-101.

[4] S.R. Johnston, M. Dowsett, Aromatase inhibitors for breast cancer: lessons from the laboratory, Nat. Rev. Cancer 3 (2003) 821-831.

[5] R.J. Santen, H. Brodie, E.R. Simpson, P.K. Siiteri, A. Brodie, History of aromatase: saga of an important biological mediator and therapeutic target, Endocr. Rev. 30 (2009) 343-375.

[6] M. Cutolo, S. Capellino, A. Sulli, B. Serioli, M.E. Secchi, B. Villaggio, R.H. Straub, Estrogens and autoimmune diseases, Ann. N. Y. Acad. Sci. 1089 (2006) 538-547.

[7] E. Murphy, Estrogen signaling and cardiovascular disease, Circ. Res. 109 (2011) 687-696.

[8] E.D. Lephart, T.D. Lund, T.L. Horvath, Brain androgen and progesterone metabolizing enzymes: biosynthesis, distribution and function, Brain. Res. Rev. 37 (2001) 25-37.

[9] H.T. Butler, D.R. Warden, E. Hogervorst, J. Ragoussis, A.D. Smith, D.J. Lehmann, Association of the aromatase gene with Alzheimer's disease in women, Neurosci. Lett. 468 (2010) 202-206.

[10] S. Catalano, A. Campana, C. Giordano, B. Győrffy, R. Tarallo, A. Rinaldi, G. Bruno, A. Ferraro, F. Romeo, M. Lanzino, F. Naro, D. Bonofiglio, S. Andò, I. Barone, Expression and function of phosphodiesterase type 5 in human breast cancer cell lines and tissues: implications for targeted therapy, Clin. Cancer Res. 22 (2015) 2271-2282.

[11] M. Sponziello, A. Verrienti, F. Rosignolo, R.F. De Rose, V. Pecce, V. Maggisano, C. Durante, S. Bulotta, G. Damante, L. Giacomelli, C.R. Di Gioia, S. Filetti, D. Russo, M. Celano, PDE5 expression in

human thyroid tumors and effects of PDE5 inhibitors on growth and migration of cancer cells, Endocrine 50 (2015) 434-441.

[12] K. Omori, J. Kotera, Overview of PDEs and their regulation, Circ. Res. 100 (2007) 309-327.

[13] Z. Shi, A.K. Tiwari, A.S. Patel, L.W. Fu, Z.S. Chen, Roles of sildenafil in enhancing drug sensitivity in cancer, Cancer Res. 71 (2011) 3735-3738.

[14] X.L. Mei, Y. Yang, Y.J. Zhang, Y. Li, J.M. Zhao, J.G. Qiu, W.J. Zhang, Q.W. Jiang, Y.Q. Xue, D.W. Zheng, Y. Chen, W.M. Qin, M.N. Wei, Z. Shi, Sildenafil inhibits the growth of human colorectal cancer in vitro and in vivo, Am. J. Cancer Res. 5 (2015) 3311-3324.

[15] E.A. Greco, M. Pili, R. Bruzziches, G. Corona, G. Spera, A. Aversa, Testosterone:estradiol ratio changes associated with long-term tadalafil administration: a pilot study, J. Sex. Med. 3 (2006) 716-722.

[16] M.M. Janjic, N.J. Stojkov, M.M. Bjelic, A.I. Mihajlovic, S.A. Andric, T.S. Kostic, Transient rise of serum testosterone level after single sildenafil treatment of adult male rats, J. Sex. Med. 9 (2012) 2534-2543.

[17] J. Lo, G. Di Nardo, J. Griswold, C. Egbuta, W. Jiang, G. Gilardi, D. Ghosh, Structural basis for the functional roles of critical residues in human cytochrome P450 aromatase, Biochemistry 52 (2013) 5821-5829.

[18] D. Ghosh, J. Griswold, M. Erman, W. Pangborn, Structural basis for androgen specificity and oestrogen synthesis in human aromatase, Nature 457 (2009) 219-223.

[19] G. Di Nardo, M. Breitner, S.J. Sadeghi, S. Castrignanò, G. Mei, A. Di Venere, E. Nicolai, P. Allegra, G. Gilardi, Dynamics and flexibility of human aromatase probed by FTIR and time resolved fluorescence spectroscopy, PLoS One 8 (2013) e82118.

[20] P. Höfer, A. Grupp, H. Nebenführ, M. Mehring, Hyperfine sublevel correlation (HYSCORE) spectroscopy: a 2D ESR investigation of the squaric acid radical, Chem. Phys. Lett. 132 (1986) 279-282.

[21] S. Stoll, A. Schweiger, EasySpin, a comprehensive software package for spectral simulation and analysis in EPR, J. Magn. Reson. 178 (2006) 42-55.

[22] G.M. Morris, D.S. Goodsell, R.S. Halliday, R. Huey, W.E. Hart, R.K. Belew, A.J. Olson, Automated docking using a Lamarckian genetic algorithm and empirical binding free energy function, J. Comput. Chem. 19 (1998) 1639-1662.

[23] S. Janocha, Y. Carius, M. Hutter, C.R. Lancaster, R. Bernhardt, Crystal structure of CYP106A2 in substrate-free and substrate-bound form, ChemBioChem. 17 (2016) 1-10.

[24] R.A. Copeland, Reversible inhibitors, in: R.A. Copeland (Ed.), Enzymes: a practical introduction to structure, mechanism and data analysis, John Wiley & Sons Inc, New York, 2000, pp 272-273.

[25] I.H. Segel, Rapid equilibrium partial and mixed-type inhibition, in: I.H. Segel (Ed.) Enzyme kinetics, Wiley, New York, 1993, pp 161-224.

[26] E. Cattaneo, L. Conti, Generation and characterization of embryonic striatal conditionally immortalized ST14A cells, J. Neurosci. Res. 53 (1998) 223-234.

[27] G. Gambarotta, D. Garzotto, E. Destro, B. Mautino, C. Giampietro, S. Cutrupi, C. Dati, E. Cattaneo, A. Fasolo, I. Perroteau, ErbB4 expression in neural progenitor cells (ST14A) is necessary to mediate neuregulin-1beta1-induced migration, J. Biol. Chem. 279 (2004) 48808-48816.

[28] I. Barone, Y. Cui, N.H. Herynk, A. Corona-Rodriguez, C. Giordano, J. Selever, A. Beyer, S. Andò, S.A.W. Fuqua, Expression of the K303R estrogen receptor α breast cancer mutation induces resistance to an aromatase via addiction to the PI3K/Akt kinase pathway, Cancer Res. 69 (2009) 4724-4732.

[29] E.D. Lephart, E.R. Simpson, Assay of aromatase activity, Methods. Enzymol. 206 (1991) 477-483.

[30] P.B. Danielson, The cytochrome P450 superfamily: biochemistry, evolution and drug metabolism in humans, Curr. Drug Metab. 3 (2002) 561-597.

[31] T.L. Poulos, B.C. Finzel, A.J. Howard, High-resolution crystal structure of cytochrome P450cam, J. Mol. Biol. 195 (1987) 687-700.

[32] K.P. Conner, P. Vennam, C.M. Woods, M.D. Krzyaniak, M.K. Bowman, W.M. Atkins, 1,2,3-triazole-heme interactions in cytochrome P450: functionally competent triazole-water-heme complexes, Biochemistry 51 (2012) 6441-6457.

[33] H.E. Seaward, A. Roujeinikova, K.J. McLean, A.W. Munro, D. Leys, Crystal structure of the Mycobacterium tuberculosis P450 CYP121-fluconazole complex reveals new azole drug-P450 binding mode, J. Biol. Chem. 281 (2006) 39437-39443.

[34] S. Maurelli, M. Chiesa, E. Giamello, G. Di Nardo, V.E.V. Ferrero, G. Gilardi, S. Van Doorslaer, Direct spectroscopic evidence for binding of anastrozole to the iron heme of human aromatase. peering into the mechanism of aromatase inhibition, Chem. Comm. (Camb.) 47 (2011) 10737-10739.

[35] J.B. Schenkman, S.G. Sligar, D.L. Cinti, Substrate interaction with cytochrome P-450, Pharmacol. Ther. 12 (1981) 43-71.

[36] G. Di Nardo, M. Breitner, A. Bandino, D. Ghosh, G.K. Jennings, J.C. Hackett, G. Gilardi, Evidence for an elevated aspartate pKa in the active site of human aromatase, J. Biol. Chem. 290 (2015) 1186-1196.

[37] S.L. Gantt, I.G. Denisov, Y.V. Grinkova, S.G. Sligar, The critical iron–oxygen intermediate in human aromatase, Biochem. Biophys. Res. Commun. 387 (2009) 169-173.

[38] K. Takeuchi, M. Tsubaki, J. Futagawa, F. Masuya, H. Hori, Adrenodoxin-cytochrome P450scc interaction as revealed by EPR spectroscopy: comparison with the putidaredoxin-cytochrome P450cam system1, J. Biochem. 130 (2001) 789-797.

[39] I. Garcia-Rubio, J.I. Martinez, R. Picorel, I.L. Yruela, P.J. Alonso, HYSCORE spectroscopy in the cytochrome b(559) of the photosystem II reaction center, J. Am. Chem. Soc. 125 (2003) 15846-15854.

[40] T.C. Yang, R.L. McNaughton, M.D. Clay, F.E. Jenney, R. Krishnan, D.M. Kurtz, M.W.W. Adams, M.K. Johnson, B.M. Hoffman, Comparing the electronic properties of the low-spin cyano-ferric [Fe(N(4))(Cys)] active sites of superoxide reductase and P450cam using ENDOR spectroscopy and DFT calculations, J. Am. Chem. Soc. 128 (2006) 16566-16578.

[41] J.T. Kellis, L.E, Vickery, Purification and characterization of human placental aromatase cytochrome P-450, J. Biol. Chem. 262 (1987) 4413-4420

[42] C.A. Gartner, S.J. Thompson, A.E. Rettie, S.D. Nelson, Human aromatase in high yield and purity by perfusion chromatography and its characterization by difference spectroscopy and mass spectrometry. (2001) Protein Expr. Purif. 22 (2001) 443-454

[43] N. Kagawa, H. Hori, M.R. Waterman, S. Yoshioka, Characterization of stable human aromatase expressed in E. coli, Steroids 69 (2004) 235-243

[44] Y. Hong, B. Yu, M. Sherman, Y. Yuan, D. Zhou, S. Chen, Molecular basis for the aromatization reaction and exemestane-mediated irreversible inhibition of human aromatase, Mol. Endocrinol. 21 (2007) 401-414

[45] C. Sohl, F. Guengerich, Kinetic analysis of the three-step steroid aromatase reaction of human cytochrome P450 19A1, J. Biol. Chem. 285 (2010) 17734-17743

[46] Y. Wang, J. Wang, Y. Cui, J.P. Fawcett, J. Gu, Liquid chromatographic-tandem mass spectrometric method for the quantitation of sildenafil in human plasma, J. Chromatogr. B. 828 (2005) 118-121.

[47] M. Al-Ghazawi, M. Tutunji, S. Aburuz, Simultaneous determination of sildenafil and N-desmethyl sildenafil in human plasma by high-performance liquid chromatography method using electrochemical detection with application to a pharmacokinetic study, J. Pharm. Biomed. Anal. 43 (2007) 613-618.

[48] J. Balthazart, G.F. Ball, Is brain estradiol a hormone or a neurotransmitter?, Trends Neurosci. 29 (2006) 241-249.

[49] C.F. Roselli, Brain aromatase: roles in reproduction and neuroprotection, J. Steroid. Biochem. Mol, Biol. 106 (2007) 143-150.

[50] S. Catalano, I. Barone, S. Marsico, R. Bruno, S. Andò, Phosphorylation processes controlling aromatase activity in breast cancer: an update, Mini-Rev. Med. Chem. 16 (2016) 691-698.

[51] A. Das, D. Durrant, F.N. Salloum, L. Xi, R.C. Kukreja, PDE5 inhibitors as therapeutics for heart disease, diabetes and cancer, Pharmacol. Ther. 147 (2015) 12-21.

Figure and Scheme Legends.

Scheme 1. Structure of substrate, products and inhibitors of human aromatase. A) The three step reaction catalysed by human aromatase; B) chemical structure of sildenafil and C) chemical structure of the aromatase inhibitor anastrozole.

Figure 2. UV-vis spectroscopy shows a Type II binding of sildenafil to human aromatase. A) Visible direct spectra of ligand-free rArom (solid black line) and in the presence of 2.5 μM of sildenafil (solid grey line). Inset: difference spectrum of rArom bound to sildenafil minus ligand-free rArom. B) Binding curve of sildenafil.

Figure 2. EPR spectroscopy shows a different binding mode of sildenafil compared to the known inhibitor anastrozole. (A) Experimental (full line) and simulated (dotted line) X-band CW-EPR of aromatase. (B) Experimental HYSCORE spectra at the field position corresponding to the arrow in (A) ($B_0 \cong 310.5$ mT). The spectra in (A) and (B) refer to frozen solutions of (a) substrate-free aromatase, (b) aromatase co-purified with anastrozole and (c) aromatase co-purified with sildenafil at pH = 7.4. The arrows in the HYSCORE spectra indicate the signals belonging to porphyrin nitrogen nuclei of heme rings and axial ligated nitrogen nuclei in anastrozole.

Figure 3. The kinetic parameters of the three steps of reaction of rArom are affected by the presence of sildenafil. rArom kinetic curves in the absence (black circles) and in the presence (grey circles) of sildenafil using as starting substrates A) androstenedione (AD), B) 19-hydroxyandrostenedione (19-OHAD) and C) 19-oxoandrostenedione (19-OXOAD). Insets show the corresponding Lineweaver-Burk linearization curves. D) Hill linearization plot for the kinetics of 19-OXOAD (data from panel C) and fitting to linear curves.

Figure 4. Sildenafil docks into the active site of human aromatase. Docking was performed in the following two conditions: A) the androstenedione substrate is removed and the pentacoordinated heme cofactor is replaced by the water-bound hexacoordinated one (red) B) the enzyme is in complex with the substrate androstenedione (blue) as in the original X-ray structure.

Figure 5. Dose-response curve for rArom activity in the presence of increasing sildenafil concentrations. Inset: Dixon plot showing a hyperbolic trend typical of partial inhibitors.

Figure 6. Western blot analysis performed on total cellular proteins extracted from ST14A neuronal cells transiently transfected with full-length aromatase and from parental MCF-7 breast cancer cells stably transfected with full-length aromatase. GAPDH was used as house-keeping protein. Purified rArom was used as positive control.

Tables.

Table 1. Kinetic parameters and inhibition constants for the three steps of reaction of rArom.

Substrate	**K_M (μM)**		**V_{max} (nmol product/min/mg protein)**		**K_{EI} (μM)**	**K_{EIS} (μM)**
	- sildenafil	+ sildenafil	- sildenafil	+ sildenafil		
AD	0.46 ± 0.06	0.65 ± 0.07	35.3 ± 0.7	30.7 ± 0.6	15.8 ± 4.5	38.5 ± 11.1
19-OHAD	4.2 ± 0.4	5.2 ± 0.6	63.6 ± 1.7	51.5 ± 1.8	18.2 ± 4.0	19.7 ± 6.7
19-OXOAD	10.2 ± 0.8	34.5 ± 0.3	210.0 ± 4.8	214.9 ± 1.4	0.11 ± 0.005	ND*

*ND = not determined

Table 2. Residual activity of full-length aromatase in ST14A and MCF-7 aromatase-expressing cells at different sildenafil concentrations.

Sildenafil concentration	Residual aromatase activity in ST14A cells (%)	p-value	Residual aromatase activity in MCF-7 cells (%)	p-value
0	100 ± 0.1		100 ± 2.8	
25 nM	88.4 ± 9.3	< 0.05	74.1 ± 7.5	< 0.05
75 nM	73.9 ± 6.1	< 0.001	73.2 ± 3.1	< 0.05
200 nM	65.1 ± 2.6	< 0.001	70.0 ± 3.0	< 0.05
1 μM	64.8 ± 0.2	< 0.001	62.0 ± 3.2	< 0.05